



---

# Enhanced CO<sub>2</sub> uptake of the coastal ocean is dominated by biological carbon fixation

---

In the format provided by the authors and unedited

## Supplementary Tables and Figures

Table S1: Simulated net CO<sub>2</sub> uptake in Pg C yr<sup>-1</sup>, integrated over the coastal, the open and the global ocean areas. The averaging period is 1991-2010 for experiments *ctrl*, *woriv* and *hist*, and the last 20 years for experiments *woriv<sub>ext</sub>* and *hist<sub>ext</sub>*.

Experiment	Coastal ocean	Open ocean	Global ocean
	Pg C yr <sup>-1</sup>	Pg C yr <sup>-1</sup>	Pg C yr <sup>-1</sup>
<i>ctrl</i>	0.10	0.58	0.68
<i>woriv</i>	0.21	1.86	2.07
<i>hist</i>	0.24	1.90	2.14
<i>woriv<sub>ext</sub></i>	0.15	1.01	1.16
<i>hist<sub>ext</sub></i>	0.19	1.04	1.23

Table S2: Comparison of NPP decadal trends of 11 satellite products and the ICON-Coast simulation *hist*. Satellite trends are calculated over the available data periods of 10-20 yr, statistical significance at the 95% level is assessed with a 2-sided t-test. Model trends are calculated over the simulation period 1900-2010.

Region	Satellite products			ICON-Coast
	trend range (g C m <sup>-2</sup> 10 yr <sup>-1</sup> )	number of sign. trends	mean, median trend (g C m <sup>-2</sup> 10 yr <sup>-1</sup> )	simulated trend (g C m <sup>-2</sup> 10 yr <sup>-1</sup> )
Global open ocean	-8 to +7	2	+1, +1	+0.6 (p<0.01)
Global coastal ocean	+1 to +34	5	+10, +5	+2.5 (p<0.01)
EBUS coastal ocean	-21 to +82	3	+19, +3	+8.9 (p<0.01)
Arctic coastal ocean	+15 to +41	11	+27, +29	+0.3 (p<0.01)

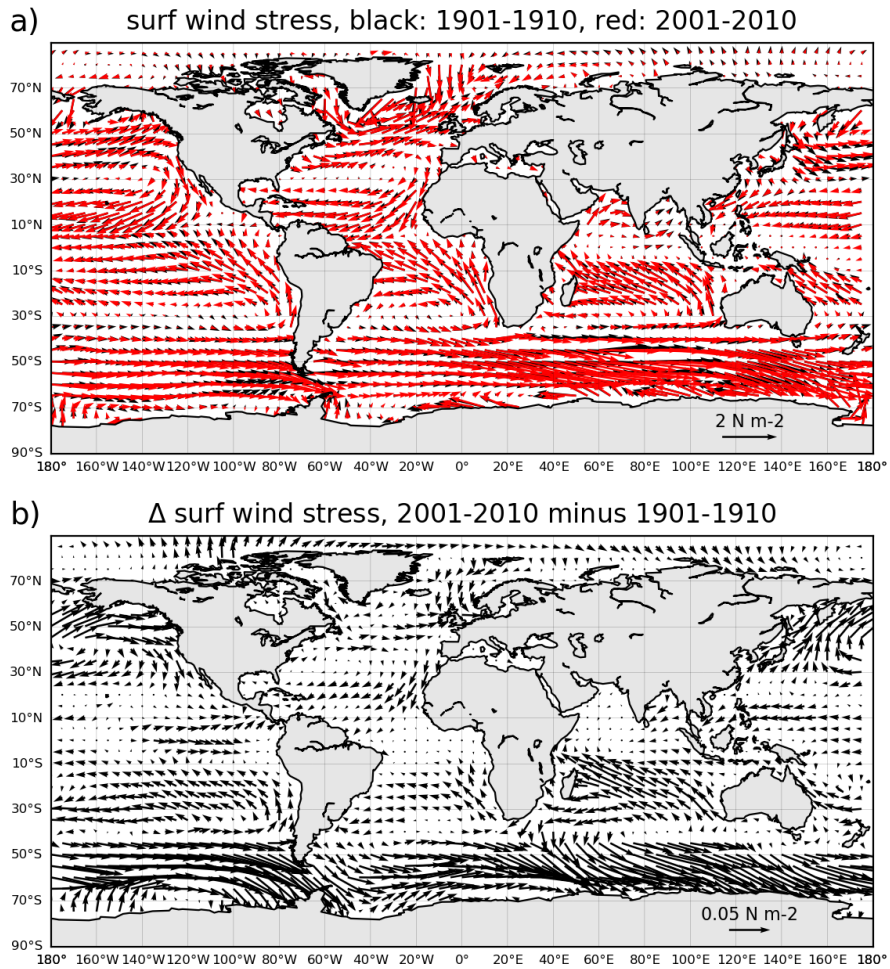


Figure S1: Ocean surface wind stress according to ERA-20C reanalysis data (Poli et al. [44,45]). In panel (a), black and red vectors show means over 1901-1910 and 2001-2010, respectively. Panel (b) shows the difference between these two periods.

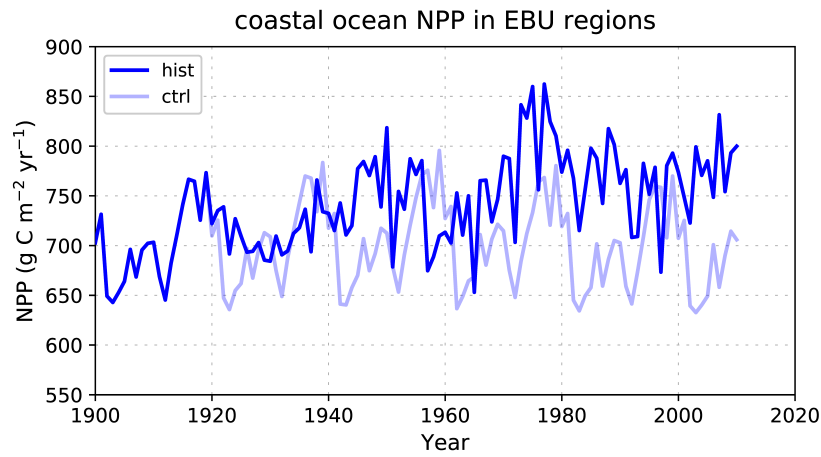


Figure S2: Simulated time series in annual NPP averaged over the coastal areas of the four eastern boundary upwelling systems: the California (20-43°N), Humboldt (8-40°S), Canary (18-43°N), and Benguela (15-32°S) current systems. Dark blue: Hindcast simulation *hist*; light blue: control simulation *ctrl*.

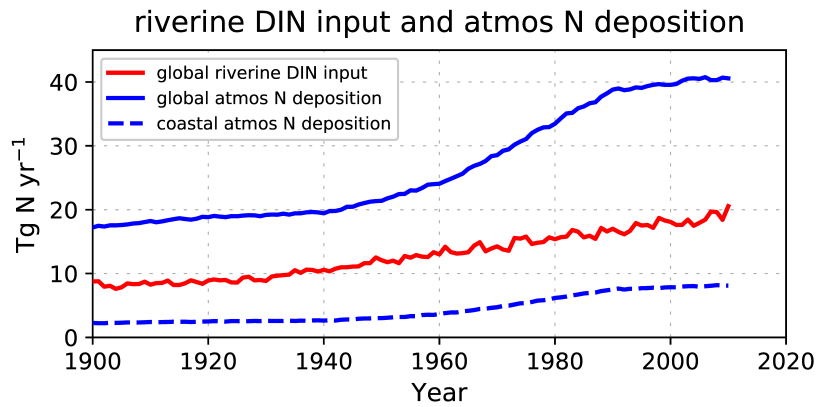


Figure S3: Prescribed nitrogen inputs from land to the ocean. Atmospheric N deposition (blue) follows Mauritsen et al. [40] and is shown for the global ocean as well as the fraction entering the coastal ocean. Riverine DIN loads (red) are derived by Lacroix et al. [11].

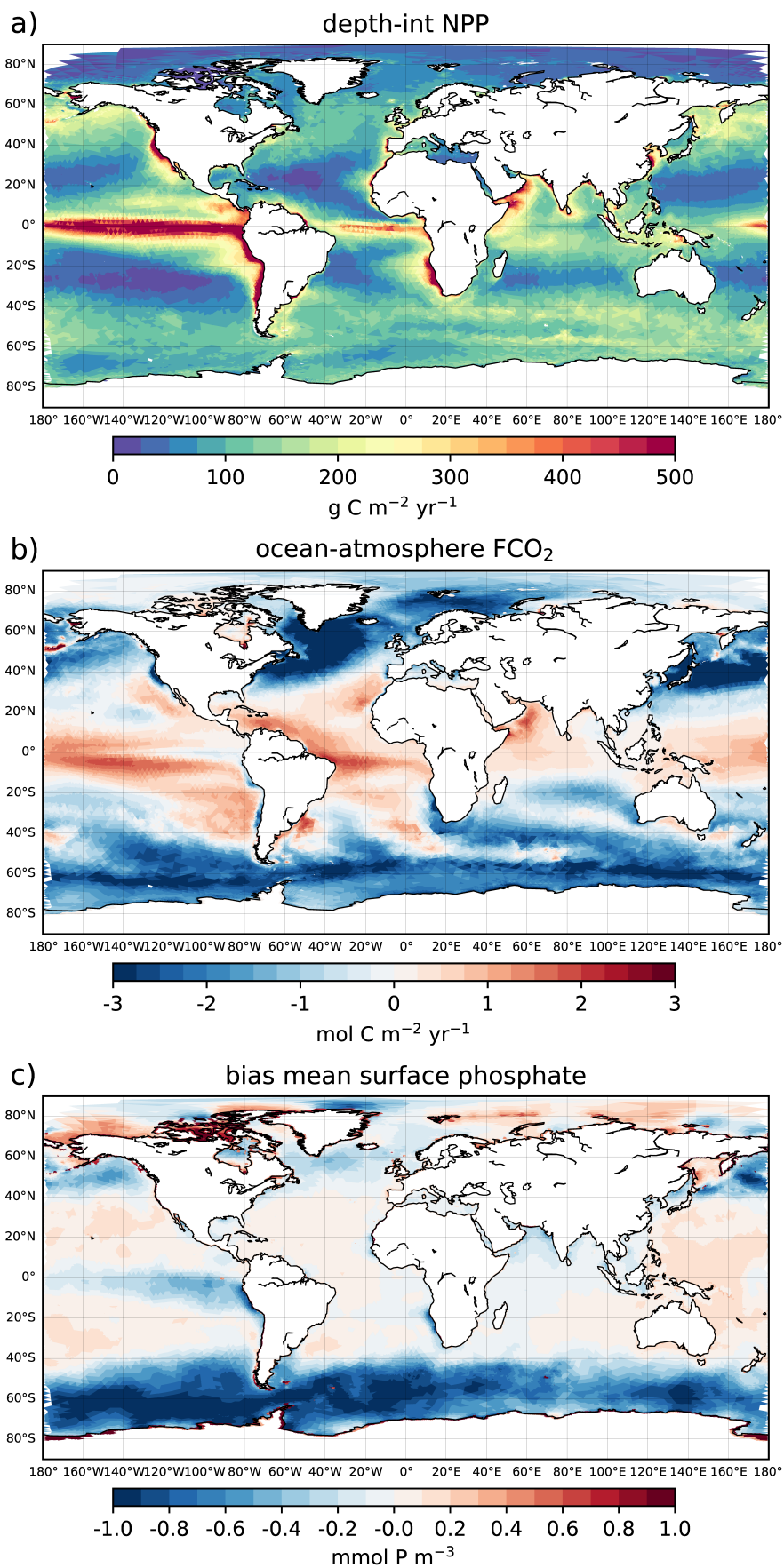


Figure S4: Global distribution of (a) depth-integrated net primary production, (b) ocean-atmosphere  $\text{CO}_2$  flux (positive means oceanic outgassing), and (c) bias of surface phosphate concentration with respect to World Ocean Atlas 2013 (Garcia et al. [52]), all simulated by ICON-Coast for the period 2001-2010 (hindcast *hist*).

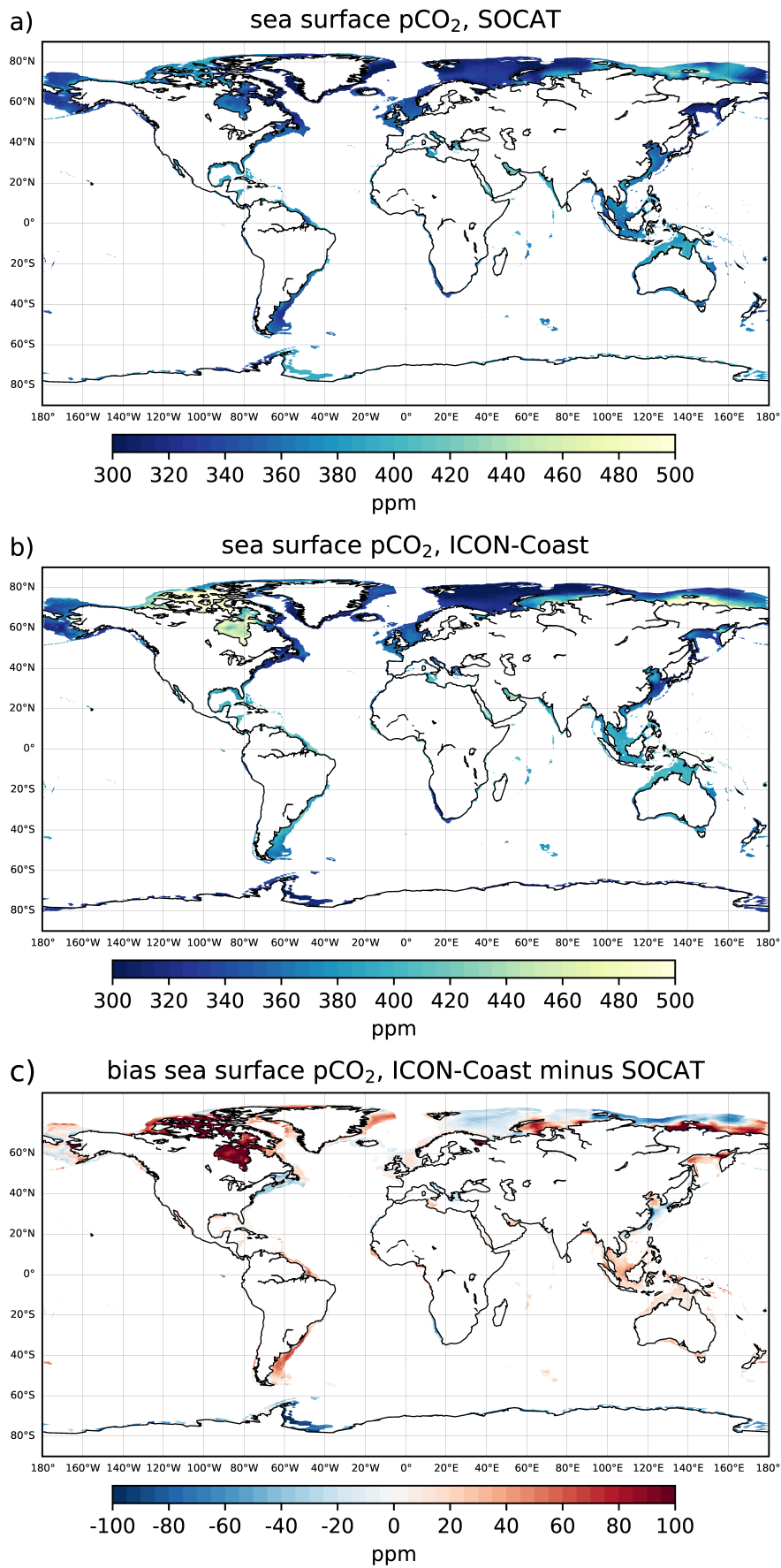


Figure S5: Comparison of climatological surface pCO<sub>2</sub> in the coastal ocean as (a) reconstructed from SOCAT data of the period 1998-2015 by Landschützer et al. [53], (b) simulated by ICON-Coast for the period 2001-2010 (hindcast *hist*), and (c) the bias of ICON-Coast.

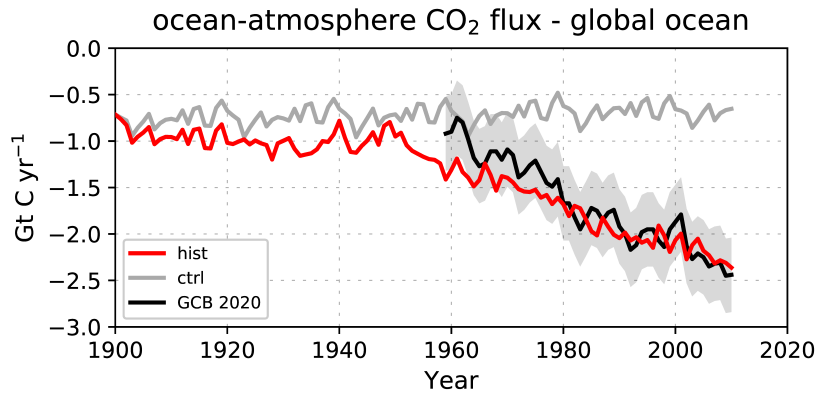


Figure S6: Comparison of simulated global ocean CO<sub>2</sub> surface flux from the hindcast *hist* with best estimates from the Global Carbon Budget (Friedlingstein et al. [32]) and associated uncertainty (shaded grey area). A negative CO<sub>2</sub> flux corresponds to oceanic uptake.

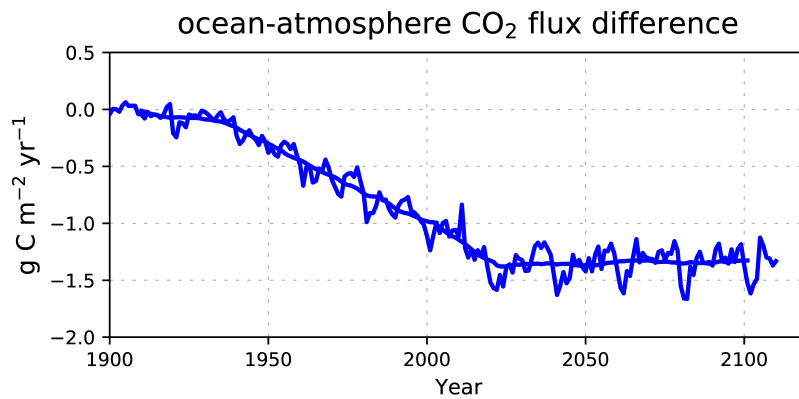


Figure S7: Difference between the coastal ocean FCO<sub>2</sub> signals of experiments *hist* and *woriv* over both, the hindcast period 1900-2010 and the subsequent 100-yr extension with constant atmospheric pCO<sub>2</sub> (*hist<sub>ext</sub>* and *woriv<sub>ext</sub>*). Time series show annual values as well as a 20-yr running mean.

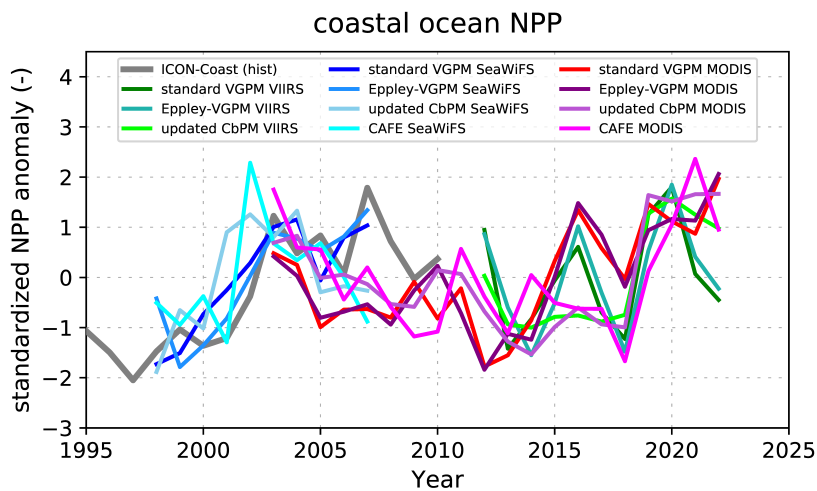


Figure S8: Simulated trends in marine NPP are reinforced by satellite-derived NPP estimates. Time series show 11 satellite products provided by the Ocean Productivity project as well as from ICON-Coast model output. All data are standardized over their individual periods to account for the high uncertainty between different imaging sensors and NPP algorithms.